International Journal on Recent and Innovation Trends in Computing and Communication
ISSN: 2321-8169 Volume: 10 Issue: 2s
DOI: https://doi.org/10.17762/ijritcc.v10i2s.5917
***Article Received**: 14 October 2022 **Revised**: 19 November 2022 **Accepted**: 22 December 2022*

ICKSC :An Efficient Methodology for Predicting Kidney Stone From CT Kidney Image Dataset using Conventional Neural Networks

J. Sarada[1], Dr. N. V. Muthu Lakshmi[2]
[1.] Research Scholar, Department of Computer Science, Sri Padmavathi Mahila Vishvavidyalayam (SPMVV), Tirupati, Andhra Pradesh – India.
[2.] Assistant Professor, Department of Computer Science, Sri Padmavathi Mahila Vishvavidyalayam (SPMVV), Tirupati, Andhra Pradesh – India.

Abstract

Chronic Kidney Diseases (CKD) has become one among the world wide health crisis and needs the associated efforts to prevent the complete organ damage. A considerable research effort has been put forward onto the effective separation and classification of kidney Stones from the kidney CT Images. Emerging machine learning along with deep learning algorithms have waved the novel paths of kidney stone detections. But these methods are proved to be laborious and its success rate is purely depends on the previous experiences. To achieve the better classification of kidney stone, this paper proposes a novel Intelligent CNN based Kidney Stone Classification (ICKSC) system which is based on transfer learning mechanism and incorporates 8 Layered CNN, densenet169_model, mobilenetv2_model, vgg19_model and xception_model. The extensive experimentation has been conducted to evaluate the efficacy of the recommended structure and matched with the other prevailing hybrid deep learning model. Experimentation demonstrates that the suggested model has showed the superior predominance over the other models and exhibited better performance in terms of training loss, accuracy, recall and precision.

Keywords: Deep learning, CNN, densenet169, mobilenetv2, vgg19, xception_model.

I. INTRODUCTION

Urolithiasis is more common than before. The presence of urinary stones is thought to be the cause of about 1.3 million visits to emergency departments [1, 2]. Although a clinical history may indicate urinary stone illness, unenhanced CT enables a precise and prompt detection [3]. These benefits have boosted CT usage for suspected urolithiasis [4, 5], but they have also enhanced imaging volume, turnaround times, the workload of radiologists, and hospital stays [6].

By using diverse imaging modalities for distinct purposes, remarkable advancements in machine learning algorithms for medical image interpretation have been made [7-9]. In the emergency department (ED), the algorithms also show promise for patient triage and optimising workflow [10, 11]. But in order for deep learning (DL) systems in medicine to work as well as possible, two significant obstacles must be overcome. The first is having access to huge, properly annotated datasets [12]. The dependability of DL models across different scanners is the second. It's possible that high-performance DL algorithms from one scanner won't work the same way when applied to another. Because of variations in collection and reconstruction procedures utilised with various imaging systems, there are discrepancies in the picture characteristics that lead to this poor generalisation [13–15].

Prior research has used transfer learning with convolutional neural network (CNN) models pretrained on a large set of natural pictures (such as ImageNet) to biomedical field despite major disparities between natural and clinical images [9, 16–17]. This is done to solve the difficulty of inadequate and unbalanced information. Models trained on datasets from the same imaging modality domain performed better for clinical uses than trained models outside of the area, according to latest studies [18, 19].

We hypothesised that DL models for CT-related tasks, including stone detection, that are pretrained on CT images may demonstrate improved generalisation. Generalization is defined as the accuracy of a model trained on pictures from one vendor and evaluated on images obtained from another vendor. It is known that transfer learning increases when characteristics between the source and target tasks are comparable [20]. To our knowledge, no research has been done on the performance of a CNN model that has been pretrained using medical photos in terms of its capacity to manage class imbalance or images from various sources [21].

We looked into the kidney stone detection capabilities of the ICKSC system using unenhanced CT images in this study. The proposed ICKSC framework used pretrained models for to prove its excellence in performance.

International Journal on Recent and Innovation Trends in Computing and Communication
ISSN: 2321-8169 Volume: 10 Issue: 2s
DOI: https://doi.org/10.17762/ijritcc.v10i2s.5917
***Article Received**: 14 October 2022 **Revised**: 19 November 2022 **Accepted**: 22 December 2022*

II. LITERATURE SURVEY

A CKD prediction approach was provided by V. Shanmugarajeshwari et al. employing three deep learning models: optimised CNN, optimised LSTM, and optimised ANN. For the kidney dataset, OCNN was determined to be the best method based on prediction accuracy, with an AUC score of 0.99 and a compilation time of 0.00447 s. The models frequently overfit because to their complex architecture. K-fold cross validation and modernised feature selection approaches are needed to address this problem [22].

An Artificial Neural Network (ANN) model was published by D. Weerasinghe et al. to identify the CKD form based on the physicochemical characteristics of the soil in agricultural regions. The results show that for identifying the illness type, the ANN model exhibits the greatest classification and prediction execution. However, this framework's main drawback is that as data size grows, more energy is consumed [23].

S. Akter et al. used ANN, LSTM, GRU, Bidirectional LSTM, Bidirectional GRU, MLP, and Simple RNN as deep learning algorithms for CKD prediction and classification. Utilizing five alternative methods to extract and assess characteristics from pre-processed and fitted CKD datasets, these algorithms were deployed based on artificial intelligence. High accuracy of 99%, 96%, and 97% was obtained by simple RNN and MLP, together with a decent prediction ratio and shorter processing time. The increased computing complexity of this system, however, is its principal drawback [24].

N. Bhaskar et al. created a more effective deep learning model that makes precise predictions by combining a bidirectional Long Short-Term Memory (LSTM) structure with a single-dimensional correlative neural network (1-D CorrNN). In order to use the strengths of both networks in the analysis of time-series data, the LSTM network and neural model are combined. In the testing dataset, this approach had an average accuracy rate of 98.08%. However, while receiving diverse input, classification time is relatively slow [25].

A Computed Tomography (CT) scan prediction model based on KNN and an edge detection system was reported by G. S. K. G. Prasad et al. utilising CT scan pictures and blood samples. When a CT or MRI scan is converted into a digital picture, edge detection is a method of image processing which is used to locate specific points or edges. In order to forecast diseases, this model employs the K-Nearest Neighbors (KNN) method. For diagnostic screening, this approach reduces costs and time. For a real-time context, extra resources are needed, albeit [26].

The objective of D. Pavithra et al. is to employ A Convolutional Neural Network (CNN) to identify CKD from clinical data. Because there are some missing values in the provided data, categorical data is imputed using the most frequent category, and numerical data is imputed using k-nearest neighbours. This framework's key advantage is that it may provide results with great accuracy while just requiring the most basic capabilities. However, training takes a lot of time [27].

The main goal of L. Antony et al. is to put several unsupervised algorithms into practise, assess how well they function, and find the best potential combinations that can boost detection rate and accuracy. This work has used five unsupervised algorithms: K-Means clustering, DB-Scan, I-Forest, and Autoencoder and they have been combined with a variety of feature selection techniques. With the K-Means clustering algorithm and feature reduction techniques combined, clinical data for CKD and non-CKD were classified with an overall accuracy of 99%. The disadvantage of this framework is that it doesn't take the computational complexity of a real-time scenario into account [28].

J. Qin et al. created a perceptron-based integrated scheme for CKD detection that integrates random forest and logistic regression. In order to handle the missing data for each incomplete sample, the K-Nearest Neighbour (KNN) assertion method was utilised, which chooses lots of full samples all comparable dimensions. The average accuracy of this framework was 99.83 percent after 10 runs. However, this framework's increased energy consumption has been identified as its main drawback [29].

A Support Vector Machine (SVM) classifier is united with a single dimensional deep learning Convolutional Neural Network (CNN) approach that was introduced and developed by N. Bhaskar et al. The condition is identified by tracking the urea levels in saliva. The CNN-SVM integrated network was used, which improved the model's classification precision. With an accuracy of 98.04%, the suggested model correctly identified the samples. But this framework's increased memory usage is considered to be its primary drawback [30].

G. Chen et al. introduced an efficient and effective Adaptive Hybridised Deep Convolutional Neural Network (AHDCNN) for the early diagnosis of renal disease. By lowering the feature dimension, this framework increased classification system accuracy, and CNN was used to create an algorithm model. The results demonstrate how this framework improved performance in terms of accuracy. In contrast, as the data size grows, the computing complexity also grows [31].

International Journal on Recent and Innovation Trends in Computing and Communication
ISSN: 2321-8169 Volume: 10 Issue: 2s
DOI: https://doi.org/10.17762/ijritcc.v10i2s.5917
***Article Received**: 14 October 2022 **Revised**: 19 November 2022 **Accepted**: 22 December 2022*

III. PROPOSED METHODOLOGY

The suggested framework's whole architecture is depicted in Figure 1. The proposed architecture's operational process is divided into four important phases. Image data preprocessing saliency segmentation, Feature extractions followed by deep feed-forward based classification layers.

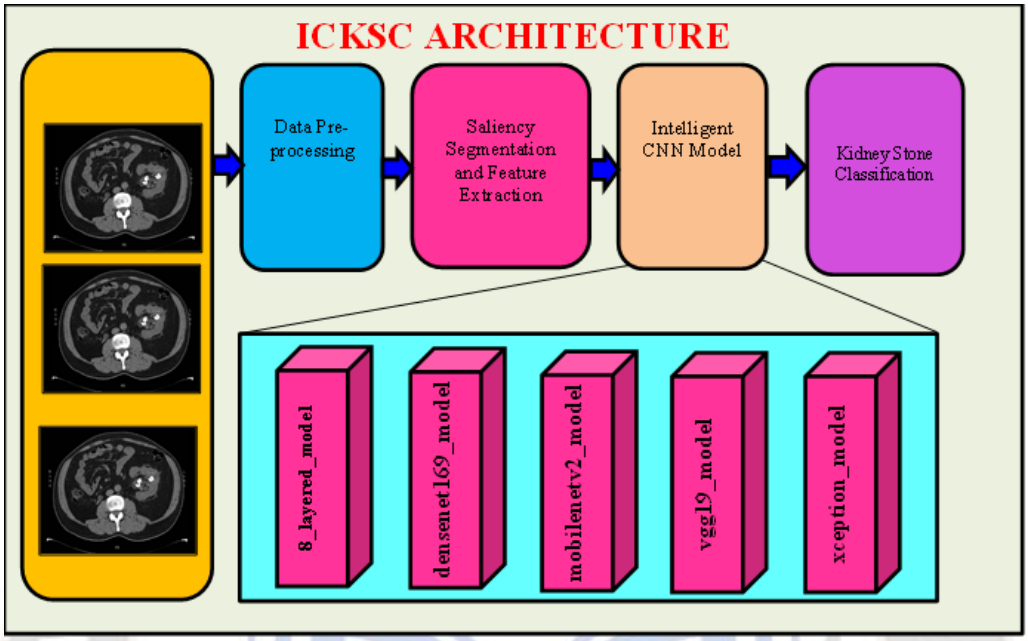

Figure 1. Proposed ICKSC architecture

3.1 Materials and Methods

This primary analysis of data here is done using Convolutional Neural Networks. From Feature Extraction to Complex Graph Networks, neural networks have a lot of advantages when it comes to classifying image data. Neural Networks, here, is also applicable due to the complex nature and volume of the data points available. The dataset has been extracted from a Kaggle Dataset (https://www.kaggle.com/code/malik12345/kidney-stone-detection-using-vgg16/notebook) and cleaned further for the model training and testing purposes. The cleaning process included balancing the dataset and later using data augmentation to increase the number of datapoints available for training.

An over all of ~12,000 images were available for training and testing/validation. Out of these, a set of ~6000 images were extracted by the already mentioned process. Speculations can be noticed on the dataset that is existence of multiple copies of the same image (duplicates).

The dataset is divided into 4 different classes – Cyst, Normal, Tumor and Stone (in Kidney(s)). Each of the Classes have 1200 images. There 70% images were utilized for training and 30% is utilized for the testing. A few other inaccuracies involved in the process include the orientation of the body during the CT Scan, evident in Figure 2.

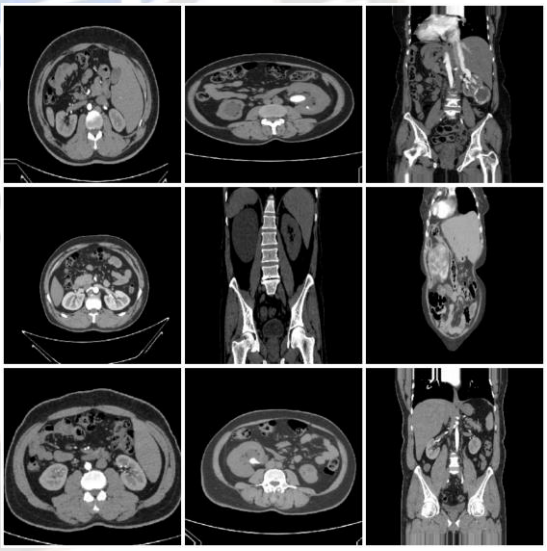

Figure 2. Ten Random Images from the Train Dataset using ImageDataGenerator

Firstly, the imbalanced dataset was let for training in a basic neural network with 5 layers. Due to the inaccuracies, the training accuracy reached ~90% while the validation accuracy became unstable at ~50% with a loss of ~7 when applied with Categorical CrossEntropy. Along with loss and accuracy, other metrics like precision and recall are also noted during the representation of training and validation per epoch. Other metrics involved in the training of this basic model are different parameters like taking the image height (150) and weight (150), channels of colors, Naïve

International Journal on Recent and Innovation Trends in Computing and Communication
ISSN: 2321-8169 Volume: 10 Issue: 2s
DOI: https://doi.org/10.17762/ijritcc.v10i2s.5917
***Article Received**: 14 October 2022 **Revised**: 19 November 2022 **Accepted**: 22 December 2022*

Bayes classifier classes set to 4, epochs set to 50 as a standard in the experimentation and a batch size of 32, initially. With the above metrics, we get an input shape of (150, 150, 3). On this basis, an input layer is generated by the tensorflow. keras module and then the data points are fed further to the consecutive layers.

An important point here to be taken is that the input shape shall be (150, 150), but that is not the shape of the image itself. Proceeding with an image data analysis, we have a report stating a majority of the images having a size of (512, 512, 3). The reason behind selecting this size is to use the data augmentation process in training and validation of the model.

3.2 Data Pre-processing:

With the intention of improving the ability to detect Kidney stones, noise and poor-quality pixels are removed from the data using the data preprocessing technique. The inconsistent pixels and noise pixels from the original kidney CT scan images are removed by the pixel intensive techniques. Additionally, image histogram techniques are used to improve the quality of the photographs because they are more effective with various types of images. The preprocessed CT kidney images are shown in Figure 3.

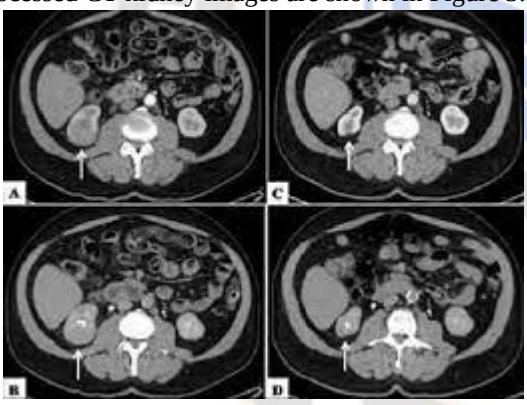

Figure 3 After Enhancement of CT Kidney Images used for kidney stone Classification

After enhancing the images, U-net visual saliency maps are used for an effective segmentation of kidney stones which are then used for feature extraction and classification.

3.3 Saliency Maps Segmentation:

3.3.1 Saliency Maps –An Overview:

Segmentation is the process of splitting images into groups using various textures and pixel values. Many techniques have been developed for segmenting the images. Here, a novel technique known as visual saliency maps descriptors has been introduced. It thoroughly breaks down each image into compact, diverse parts. The photographs will be edited to remove any extraneous details.

Color & spatial differences are employed in a pixel based computing, where every pixel is denoted as a block, to generate saliency models[21]. To do this, the pixels "X" are scaled to 256x256, and after that, they are divided into non-overlying blocks of dimension n x n, where n=8 & 16. Therefore, the mathematical equations provided by are used to calculate the saliency maps M(s).

$$\mathrm{M}(s) = \sum_{k=8,16} \quad X(k) * M'(s) \qquad (1)$$

As noted in [21], the final saliency maps are derived as the weighted sum of the actual (M(s)), previous (M (S1)), and next blocks (M(S2)) color and spatial saliency. This is because the position, size, & shape of kidney stone are fairly similar in surrounding clippings.

$$M(s) = w1 * M(m_1) + w2 * M(s) + w * M(s2) \qquad (2)$$

The refinement of segmentation images requires the use of post-processing techniques once the saliency maps have been calculated. Active contour methods are adapted for all extraction of the saliency counters which leads to the high complexity in terms of computational overhead. To overcome this drawback, this research proposes the ICKSC for the better contour extraction.

3.3.2 Proposed Saliency Segmentation and Feature Extraction Module

In the first stage, the finer segmentation of saliencies is done from the CT images. The saliency maps are segmented by using this proposed network and it is extremely useful for a better segmentation of images even it is smaller and also avoids the problem of overfitting. After segmenting the saliency maps, feature extraction layers are formed by CNN Layers.

3**.4 Model Training Layers**

After the feature extracted which are then feed for training the networks intelligent CNN network. This network comprises of the following pretrained models.

- 8 Layered CNN Model using keras layers
  - Layers – Dense, Conv2D
  - Activation Functions – Relu, Softmax
- VGG19
- DenseNet169
- MobileNetV2
- Xception

3.5 Convolutional Neural Networks

Multi-Layer Perceptron (MLP) technology has been improved by convolutional neural network (CNN), which is driven by biology. When characterising images, grouping images, and identifying objects in images, CNN is frequently used. They are also used for handling regular

International Journal on Recent and Innovation Trends in Computing and Communication
ISSN: 2321-8169 Volume: 10 Issue: 2s
DOI: https://doi.org/10.17762/ijritcc.v10i2s.5917
***Article Received**: 14 October 2022 **Revised**: 19 November 2022 **Accepted**: 22 December 2022*

languages and optical character recognition. CNNs may be used to analyse sound in addition to images when viewed as a spectrogram. Additionally, CNN has been used directly for message analysis, just like convolutional neural networks are used for chart information. When measured against its gauge calculations, CNN's degree of craftsmanship and craftsmanship skill enable it to be successful across a range of industries. Channels, often referred to as bits, and are used by CNN to identify the highlights, as seen in Figure 4. A network of attributes that have been loaded to differentiate explicit highlights is what makes up a channel. Convolution is a component insightful action that is completed between two networks, and it can be performed via the channel.

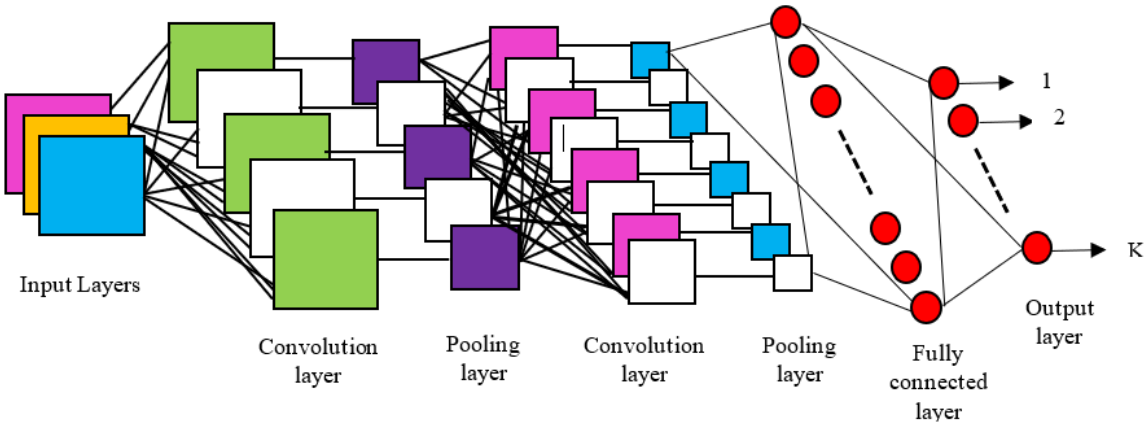

Figure 4: Schematic representation of convolutional neural networks.

The CNN's preparation is ensured by reducing the amount of recurrence in the information highlight. As a consequence, the organisation uses less memory. Max pooling is a simple method to do this, in which a window ignores input data and a yield framework is built using the window's highest value as a pool. Connecting convolution layers with max pooling jobs makes the computation effective for extraction. In order to deliver the element maps, the input is processed through these deep layers, and then an MLP is used to transform the element maps into element vectors. In the created model, this is referred to as an "eight-layered" model that facilitates high-level reasoning. The following Figure 5 represents the how images are fed into CNN model.

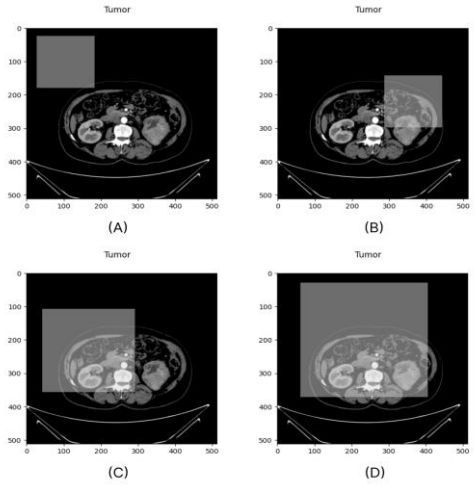

Figure 5. Representation of how images are fed into CNN Models.

Anyhow, from the above image we can note that the images have some complexities, wherein the images represented in Figure 5 cannot be used for training on an input shape of (150, 150, 3). The reason behind, in Figure 5 (B) the transparent grey square represents the input (randomly chosen) data point does carry forward the features of the image. Whereas in Figure 5 (A), the grey colored section does not carry any features useful for training. And thus, we further went over using the image sizes of (244, 244, 3) and (299, 299, 3) based on the compatibility of the models input (Figure 5(C)(D)).

3.6 VGG-19 Models

Our classification model uses very deep convolutional networks because they achieve a substantial level of accuracy on picture classification and localization tasks, which makes them ideal for large-scale image recognition. We used it for our research because of its innate ability to process CT image recognition.

3.7 DenseNet169

DenseNet, which establishes feed-forward connections between all layers. All previous layers' feature maps are utilised as inputs for each layer, and each layer's own feature maps are used as inputs for all succeeding levels. DenseNets offer a lot of compelling benefits: they solve the vanishing-gradient issue, improve feature propagation, promote feature reuse, and drastically reduce the number of parameters. The memory and processing requirements for DenseNets are lower.

International Journal on Recent and Innovation Trends in Computing and Communication
ISSN: 2321-8169 Volume: 10 Issue: 2s
DOI: https://doi.org/10.17762/ijritcc.v10i2s.5917
***Article Received**: 14 October 2022 **Revised**: 19 November 2022 **Accepted**: 22 December 2022*

3.8 MobileNetV2

A trained model for classifying images is called MobilenetV2. Deep neural networks that have been pre-trained on a big picture dataset are known as pre-trained models. The distinctive feature of the MobileNetV2 design is how little processing power is needed for it to operate. The deep neural network is substantially simpler and contains fewer parameters. Deep neural networks become more portable as a result. It now has much more effectiveness and strength as a result. Because they are smaller and simpler, the MobileNetV2 models run quicker.

3.9 Xception

Xception is an extension of the Inception architecture which replaces the standard Inception modules with depth wise separable convolutions. With residual connections to decrease time and space complexity, Xception is developed on Inception-V3 and uses a linear stack of depth-wise separable convolution layers.

IV. RESULTS AND DISCUSSION

The experimentation involves the testing of the proposed architecture in which the saliency segmented maps are used as the inputs to the feature layers and deep feed forward training networks that classifies the Kidney stone. Metrics including accuracy (Acc), sensitivity (Sen), specificity (Spec), Precision (Pre), and f1-score are calculated to assess the effectiveness of the suggested design. Table 5 displays the computation formulas for the metrics used to evaluate the proposed architecture.

Table 5 Mathematical Equations for the calculation of specifications

S.NO	Specifications	Mathematical Equations
01	Accuracy (Acc)	$\frac{TP+TN}{TP+TN+FP+FN}$
02	Sensitivity (Sen)	$\frac{TP}{TP+FN}$ x100
03	Specificity (Spec)	$\frac{TN}{TN+FP}$
04	Precision (Pre)	$\frac{TN}{TP+FP}$
05	F1-Score	$2.\frac{Precison * Recall1}{Precision + Recall1}$

Where, TP ⇨ True Positive Values,
TN ⇨True Negative Values,
FP ⇨ False Positive
FN ⇨ False negative values

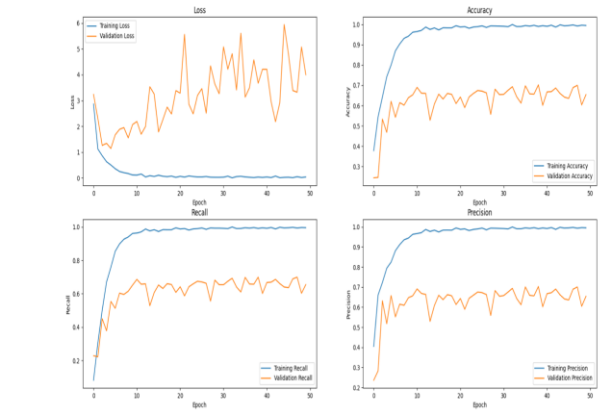

Figure 6. **8_layered_model** training and validation metrics stacked together

From the 5_layered_model trained with the uncleaned dataset, we received an accuracy of ~50% and loss ~7. Due to which the dataset has been modified with the features already mentioned, i.e., 1200 images for each class. Images fed to the CNN Model are received through the ImageDataGenerator pipeline from tensorflow.keras.preprocessing.image module. Firstly, this data set was fed into the 8_layered_model using weights of the imagenet standard using the vgg16 preprocessing function on the image. Upon comparison with/without the preprocessing function, we come to a conclusion that the preprocessing did not put changes in feature extraction. Although, processing of images using Otsu's Binarization [33] may help in extracting more features.

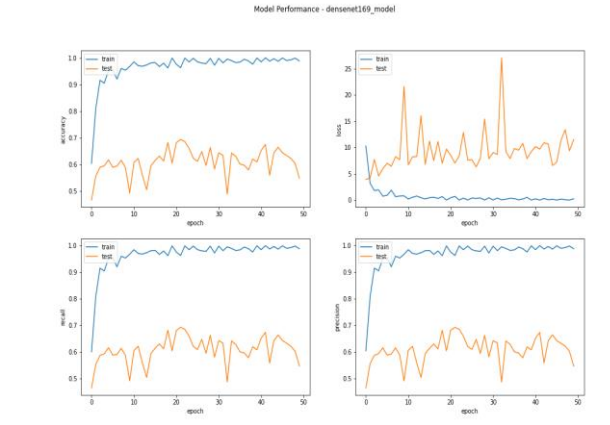

Figure 7. **densenet169_model** training and validation metrics stacked together

The 8_layered_model was based on the sequential module from the keras library and the other state of the art models are imported from the TensorFlow Library. All the 5 modules have been compiled with the loss function – Categorical Cross Entropy, optimizer - RMSProp with a

International Journal on Recent and Innovation Trends in Computing and Communication
ISSN: 2321-8169 Volume: 10 Issue: 2s
DOI: https://doi.org/10.17762/ijritcc.v10i2s.5917
***Article Received**: 14 October 2022 **Revised**: 19 November 2022 **Accepted**: 22 December 2022*

learning rate of 0.001, and extracting the accuracy, recall and precision metrics for both training and validation.

From analysis of the graphs obtained by training the 5 models, we get the results in Figure 7-10. Image input shape of (244, 244, 3) was used in training of the 8_layered_model, vgg19_model, densenet169_model, whereas the input shape of (299, 299, 3) was used in the training of xception_model and mobilenetv2_model. Noticeable observations are the 8_layered_model and vgg19_model have comparatively performed well in terms of both loss and accuracy metrics. While we notice inconsistencies in the accuracies and losses of the training in densenet169_model, mobilenetv2_model and xception_model.

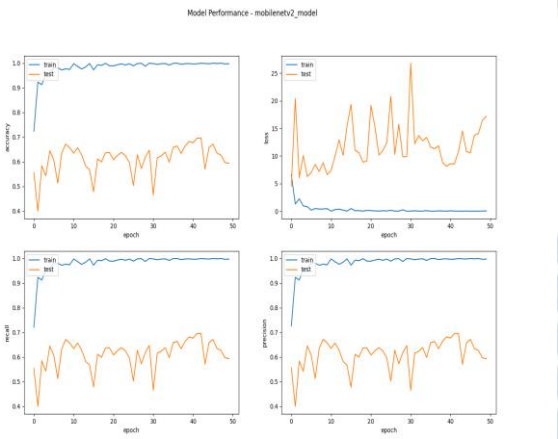

Figure 8. **mobilenetv2_model** training and validation metrics stacked together

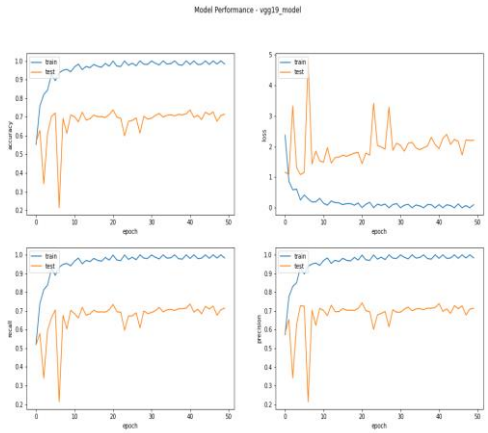

Figure 9. **vgg19_model** training and validation metrics stacked together

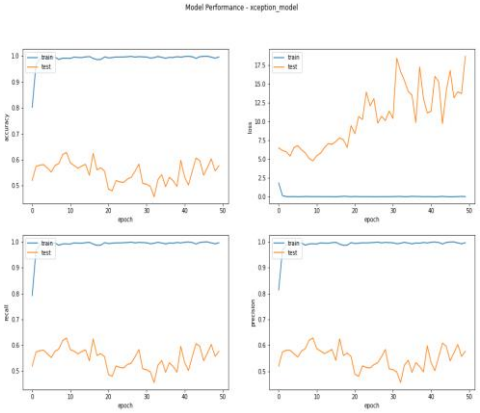

Figure 10. **xception_model** training and validation metrics stacked together

Training metrics (Figure 11) shown below is the depiction, that these metrics would not add much factor in our experimentation. Although a noticeable observation is the inconsistency noted in xception_model during the training process. Further down the experimentation, we come to a result where the inconsistencies of densenet169, mobilenetv2 and xception are very close by getting the Standard Deviations of validation loss metrics (Figure 12).

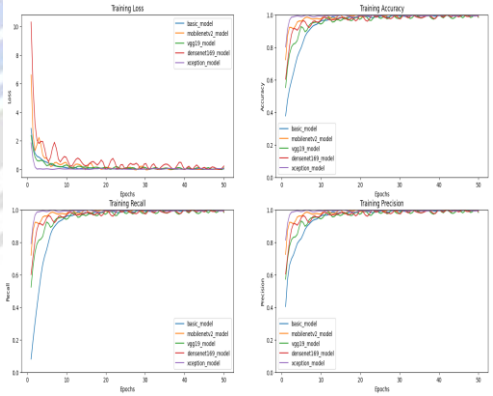

Figure 11. Comparative Analysis of different models' training metrics

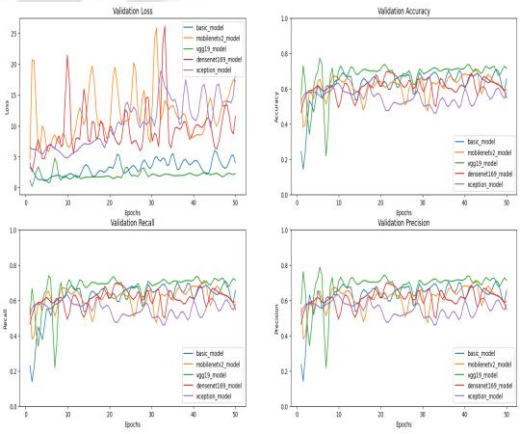

Figure 12. Comparative Analysis of different models' validation metrics

International Journal on Recent and Innovation Trends in Computing and Communication
ISSN: 2321-8169 Volume: 10 Issue: 2s
DOI: https://doi.org/10.17762/ijritcc.v10i2s.5917
***Article Received**: 14 October 2022 **Revised**: 19 November 2022 **Accepted**: 22 December 2022*

Studying the metrics further, we come to a conclusion that 8_layered_model have a very similar pattern during the training and validation of the dataset. From Figure 13 (A) and Figure 13 (B), it is evident that the accuracy and loss has been consistent throughout the training process and have very similar accuracy and SD of loss metrics, respectively.

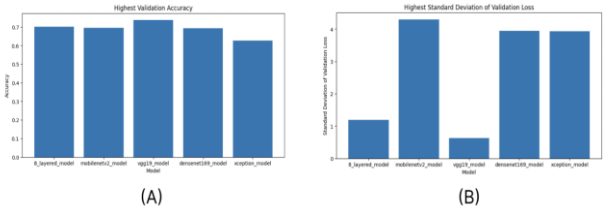

Figure 13. Comparative Analysis of 5 models (A) Validation Accuracy Peak for each model (B) Standard Deviation between losses for each model

Although, to verify this observation, we build a Correlation Matrix (Figure 14) to identify any similarities during the validation at each epoch. In the result, we notice that the relation between the 8_layered_model and mobilenetv2_model was stronger than the relation between 8_layered_model and vgg19_model. Due to the slight increase in accuracy, we cannot term VGG19 as a better classifier for the taken Kidney CT Scan Dataset but through the lesser SD in losses, we term VGG19 to be a better classifier. This classification can be improved in both the 8_layered and the VGG19 by removing the inconsistencies in the dataset, but due to the correlation of the performance between MobileNetV2 Model and the 8_Layered_Model, we cannot assure that it can perform better than the VGG19 Model. With a much larger dataset, this accuracies can be increased with the same parameters used as the model (VGG19, 8 Layered CNN Model) because they worked significantly well in a imbalanced dataset.

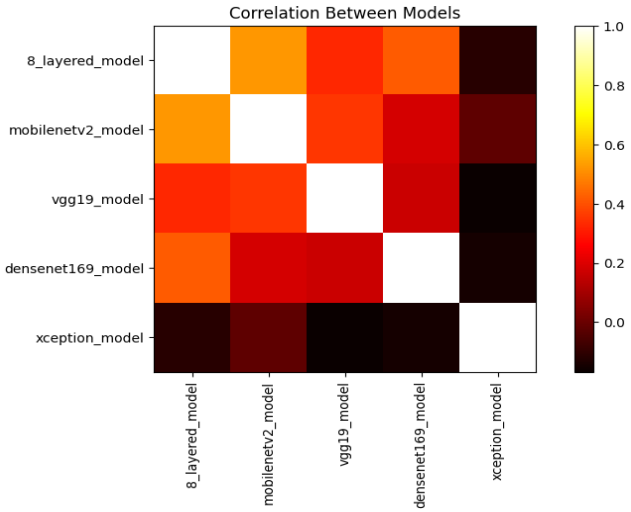

Figure 14. Correlation between multiple models on the basis of validation accuracies

The Figure 15 gives the computational time analysis for the proposed model in kidney stone detection.

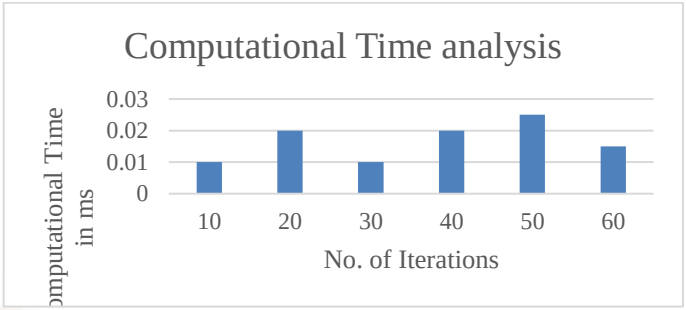

Figure 15. Computational time of the Proposed architecture (**ICKSC)** with different Epochs

The Figure 15 shows the computational time analysis of the proposed architecture **ICKSC**. From this figure, it is clear that the proposed framework require less computation time which is in the range of (0.01ms to 0.025ms) for the kidney stone detection because it utilized the pretrained models for the kidney stone detection.

V. CONCLUSION

The vital objective of this investigation is to find and classify the kidney stones using CT Scan Images .To accomplish this objective, the paper proposes ICKSC framework which comprises of saliency based segmentations and CNN (8 Layered CNN Model, VGG19, DenseNet169, MobileNetV2, Xception model). The proposed saliency model is used for segmentation whereas CNN layers are used for the classification. The comprehensive experimentation has been conducted and evaluated the efficacy of the suggested illustration with the standard architectures. The outcome demonstrates that the suggested architecture surpassed other state-of-the-art architectures and achieved maximum results, including accuracy, sensitivity and specificity, precision, and F1-score. In the future, larger real-time clinical datasets will need to be used for more rigorous testing. Additionally, the suggested approach requires improvement in order to reduce computing overhead, which will be crucial for the timely diagnosis and effective treatment of kidney stones in clinical settings.

REFERENCES

[1]. Chen Z, Prosperi M, Bird VY. Prevalence of kidney stones in the USA: the National Health and Nutrition Evaluation Survey. J Clin Urol 2018 Nov 26 [Epub ahead of print] https://doi.org/10.1177/2051415818813820.

[2]. Foster G, Stocks C, Borofsky MS. Emergency Department Visits and Hospital Admissions for Kidney Stone Disease, 2009: Statistical Brief #139. Healthcare Cost and Utilization Project (HCUP) Statistical Briefs.

International Journal on Recent and Innovation Trends in Computing and Communication
ISSN: 2321-8169 Volume: 10 Issue: 2s
DOI: https://doi.org/10.17762/ijritcc.v10i2s.5917
***Article Received**: 14 October 2022 **Revised**: 19 November 2022 **Accepted**: 22 December 2022*

Rockville, Md: Agency for Healthcare Research and Quality, 2012. https://www.ncbi. nlm.nih.gov/pubmed/23016164. Accessed February 16, 2019.

[3]. American College of Radiology. ACR appropriateness criteria. Acute onset flank pain-suspicion of stone disease (urolithiasis). https://acsearch.acr.org/ docs/69362/Narrative/. Accessed February 12, 2019.

[4]. Westphalen AC, Hsia RY, Maselli JH, Wang R, Gonzales R. Radiological imaging of patients with suspected urinary tract stones: national trends, diagnoses, and predictors. Acad Emerg Med 2011;18(7):699–707.

[5]. Fwu CW, Eggers PW, Kimmel PL, Kusek JW, Kirkali Z. Emergency department visits, use of imaging, and drugs for urolithiasis have increased in the United States. Kidney Int 2013;83(3):479–486.

[6]. Wang DC, Parry CR, Feldman M, Tomlinson G, Sarrazin J, Glanc P. Acute abdomen in the emergency department: is CT a time-limiting factor? AJR Am J Roentgenol 2015;205(6):1222–1229.

[7]. Lee H, Tajmir S, Lee J, et al. Fully automated deep learning system for bone age assessment. J Digit Imaging 2017;30(4):427–441.

[8]. Prevedello LM, Erdal BS, Ryu JL, et al. Automated critical test findings identification and online notification system using artificial intelligence in imaging. Radiology 2017;285(3):923–931.

[9]. Lakhani P, Sundaram B. Deep learning at chest radiography: automated classification of pulmonary tuberculosis by using convolutional neural networks. Radiology 2017;284(2):574–582.

[10]. Levin S, Toerper M, Hamrock E, et al. Machine-learning-based electronic triage more accurately differentiates patients with respect to clinical outcomes compared with the emergency severity index. Ann Emerg Med 2018;71(5):565–574.e2.

[11]. Berlyand Y, Raja AS, Dorner SC, et al. How artificial intelligence could transform emergency department operations. Am J Emerg Med 2018;36(8):1515–1517.

[12]. Greenspan H, van Ginneken B, Summers RM. Guest editorial: Deep learning in medical imaging: overview and future promise of an exciting new technique. IEEE Trans Med Imaging 2016;35(5):1153–1159.

[13]. AlBadawy EA, Saha A, Mazurowski MA. Deep learning for segmentation of brain tumors: Impact of cross-institutional training and testing. Med Phys 2018;45(3):1150–1158.

[14]. Cole JH, Poudel RPK, Tsagkrasoulis D, et al. Predicting brain age with deep learning from raw imaging data results in a reliable and heritable biomarker. Neuroimage 2017;163:115–124.

[15]. Mordang JJ, Janssen T, Bria A, Kooi T, Gubern-Merida A, Karssemeijer N. Automatic microcalcification detection in multi-vendor mammography using convolutional neural networks. In: Tingberg A, Lang K, Timberg P, eds. Breast Imaging. IWDM 2016. Lecture Notes in Computer Science, vol 9699. Cham, Switzerland: Springer International, 2016; 35–42.

[16]. Esteva A, Kuprel B, Novoa RA, et al. Dermatologist-level classification of skin cancer with deep neural networks. Nature 2017;542(7639):115–118 [Published correction appears in Nature 2017;546(7660):686.] https://doi. org/10.1038/nature21056.

[17]. K., Samunnisa & MALOTH, BHAV SINGH. (2016). Privacy-Preserving Scalar Product Computation over Personal Health Records. International Journal of Computer Engineering In Research Trends. 3. 42-46.

[18]. Amit G, Ben-Ari R, Hadad O, Monovich E, Granot N, Hashoul S. Classification of breast MRI lesions using small-size training sets: comparison of deep learning approaches. In: Armato S III, Petrick NA, eds. Proceedings of SPIE: medical imaging 2017—computer-aided diagnosis. Vol 10134. Bellingham, Wash: International Society for Optics and Photonics, 2017; 101341H.

[19]. Kim HG, Choi Y, Ro YM. Modality-bridge transfer learning for medical image classification. 2017 10th International Congress on Image and Signal Processing, BioMedical Engineering and Informatics (CISP-BMEI), 2017; 1–5.

[20]. Reddy, V. & Priya, B. & Vinuthna, P. & Reddy, K. & Reddy, D.. (2022). Exploration of Image Inpainting approaches and challenges: A Survey. International Journal of Computer Engineering in Research Trends. 9. 79-92. 10.22362/ijcert/2022/v9/i05/v9i0501.

[21]. Shin HC, Roth HR, Gao M, et al. Deep convolutional neural networks for computer-aided detection: CNN architectures, dataset characteristics and transfer learning. IEEE Trans Med Imaging 2016;35(5):1285–1298

[22]. V. Shanmugarajeshwari and M. Ilayaraja, "Chronic Kidney Disease for Collaborative Healthcare Data Analytics using Random Forest Classification Algorithms," 2021 International Conference on Computer Communication and Informatics (ICCCI), 2021, pp. 1-14, doi: 10.1109/ICCCI50826.2021.9402574.

[23]. D. Weerasinghe, B. T. G. S. Kumara, B. Kuhaneswaran and S. K. Gunathilake, "Identifying the Type of Chronic Kidney Disease Based on Heavy Metals in Soil using ANN," 2021 Third International Sustainability and Resilience Conference: Climate Change, 2021, pp. 270-274, doi: 10.1109/IEEECONF53624.2021.9667974.

[24]. Velugoti, Swathi & Reddy, Revuri & Tarannum, Sadiya & Reddy, Sama. (2022). Lung Nodule Detection and Classification using Image Processing Techniques. International Journal of Computer Engineering in Research Trends. 9. 114-119. 10.22362/ijcert/2022/v9/i07/v9i0701.

[25]. N. Bhaskar, M. Suchetha and N. Y. Philip, "Time Series Classification-Based Correlational Neural Network With Bidirectional LSTM for Automated Detection of Kidney Disease," in IEEE Sensors Journal, vol. 21, no. 4, pp.

4811-4818, 15 Feb.15, 2021, doi: 10.1109/JSEN.2020.3028738.

[26]. G. S. K. G. Prasad, A. A. Chowdari, K. P. Jona and R. Senapati, "Detection of CKD from CT Scan images using KNN algorithm and using Edge Detection," 2022 2nd International Conference on Emerging Frontiers in Electrical and Electronic Technologies (ICEFEET), 2022, pp. 1-4, doi: 10.1109/ICEFEET51821.2022.9848173.

[27]. D. Pavithra and R. Vanithamani, "Chronic Kidney Disease Detection from Clinical Data using CNN," 2021 IEEE International Conference on Distributed Computing, VLSI, Electrical Circuits and Robotics (DISCOVER), 2021, pp. 282-285, doi: 10.1109/DISCOVER52564.2021.9663670.

[28]. L. Antony et al., "A Comprehensive Unsupervised Framework for Chronic Kidney Disease Prediction," in IEEE Access, vol. 9, pp. 126481-126501, 2021, doi: 10.1109/ACCESS.2021.3109168.

[29]. J. Qin, L. Chen, Y. Liu, C. Liu, C. Feng and B. Chen, "A Machine Learning Methodology for Diagnosing Chronic Kidney Disease," in IEEE Access, vol. 8, pp. 20991-21002, 2020, doi: 10.1109/ACCESS.2019.2963053.

[30]. N. Bhaskar and S. Manikandan, "A Deep-Learning-Based System for Automated Sensing of Chronic Kidney Disease," in IEEE Sensors Letters, vol. 3, no. 10, pp. 1-4, Oct. 2019, Art no. 7001904, doi: 10.1109/LSENS.2019.2942145.

[31]. G. Chen et al., "Prediction of Chronic Kidney Disease Using Adaptive Hybridized Deep Convolutional Neural Network on the Internet of Medical Things Platform," in IEEE Access, vol. 8, pp. 100497-100508, 2020, doi: 10.1109/ACCESS.2020.2995310.

[32]. D. Liu and J. Yu, "Otsu Method and K-means," 2009 Ninth International Conference on Hybrid Intelligent Systems, 2009, pp. 344-349, doi: 10.1109/HIS.2009.